



This is a repository copy of *Improved ambient stability of thermally annealed zinc nitride thin films*.

White Rose Research Online URL for this paper:
<http://eprints.whiterose.ac.uk/159365/>

Version: Published Version

Article:

Trapalis, A. orcid.org/0000-0003-4887-7058, Farrer, I. orcid.org/0000-0002-3033-4306, Kennedy, K. et al. (3 more authors) (2020) Improved ambient stability of thermally annealed zinc nitride thin films. *AIP Advances*, 10 (3). 035018.

<https://doi.org/10.1063/1.5144054>

Reuse

This article is distributed under the terms of the Creative Commons Attribution (CC BY) licence. This licence allows you to distribute, remix, tweak, and build upon the work, even commercially, as long as you credit the authors for the original work. More information and the full terms of the licence here:
<https://creativecommons.org/licenses/>

Takedown

If you consider content in White Rose Research Online to be in breach of UK law, please notify us by emailing eprints@whiterose.ac.uk including the URL of the record and the reason for the withdrawal request.



eprints@whiterose.ac.uk
<https://eprints.whiterose.ac.uk/>

Improved ambient stability of thermally annealed zinc nitride thin films

Cite as: AIP Advances **10**, 035018 (2020); <https://doi.org/10.1063/1.5144054>

Submitted: 02 January 2020 . Accepted: 26 February 2020 . Published Online: 13 March 2020

A. Trapalis , I. Farrer , K. Kennedy , A. Kean, J. Sharman, and J. Heffernan 



View Online



Export Citation



CrossMark

ARTICLES YOU MAY BE INTERESTED IN

[Achieving non-degenerate Zn₃N₂ thin films by near room temperature sputtering deposition](#)

Applied Physics Letters **115**, 092104 (2019); <https://doi.org/10.1063/1.5101037>

[Suppressing the carrier concentration of zinc tin nitride thin films by excess zinc content and low temperature growth](#)

Applied Physics Letters **115**, 232104 (2019); <https://doi.org/10.1063/1.5129879>

[Development of microLED](#)

Applied Physics Letters **116**, 100502 (2020); <https://doi.org/10.1063/1.5145201>



NEW

AVS Quantum Science

A new interdisciplinary home for impactful quantum science research and reviews

Co-Published by



NOW ONLINE

Improved ambient stability of thermally annealed zinc nitride thin films

Cite as: AIP Advances 10, 035018 (2020); doi: 10.1063/1.5144054

Submitted: 2 January 2020 • Accepted: 26 February 2020 •

Published Online: 13 March 2020



View Online



Export Citation



CrossMark

A. Trapalis,^{1,a)} I. Farrer,¹ K. Kennedy,² A. Kean,³ J. Sharman,³ and J. Heffernan¹

AFFILIATIONS

¹Department of Electronic and Electrical Engineering, University of Sheffield, North Campus, Broad Lane, Sheffield S3 7HQ, United Kingdom

²Nanofabrication Core Lab, King Abdullah University of Science and Technology, Thuwal 23955-6900, Kingdom of Saudi Arabia

³Johnson Matthey, Blount's Court, Reading RG4 9NH, United Kingdom

^{a)} Author to whom correspondence should be addressed: a.trapalis@sheffield.ac.uk

ABSTRACT

Zinc nitride films are known to readily oxidize in an ambient atmosphere, forming a ZnO/Zn(OH)₂ medium. We report that post-growth thermal annealing significantly improves the stability of zinc nitride with a three-order magnitude increase in degradation time from a few days in un-annealed films to several years after annealing. A degradation study was performed on samples annealed under a flow of nitrogen at 200–400 °C, which showed that the stability of the films depends strongly on the annealing temperature. We propose a mechanism for this improvement, which involves a stabilization of the native oxide layer that forms on the surface of zinc nitride films after exposure to ambient conditions. The result holds significant promise for the use of zinc nitride in devices where operational stability is a critical factor in applications.

© 2020 Author(s). All article content, except where otherwise noted, is licensed under a Creative Commons Attribution (CC BY) license (<http://creativecommons.org/licenses/by/4.0/>). <https://doi.org/10.1063/1.5144054>

INTRODUCTION

Zinc nitride (Zn₃N₂) is a less-studied II–V semiconductor material that has recently gained attention in the search of earth-abundant materials as candidates for the development of low-cost semiconductor devices.^{1–12} The scientific literature has yet to reach a consensus regarding some of the properties of Zn₃N₂. For instance, some studies have reported a narrow bandgap in Zn₃N₂ films, making this material suitable for use as a solar absorber,^{9,13–23} while others report a wide bandgap, which could make Zn₃N₂ viable as a transparent conductive nitride.^{1,6,24–31} However, it is known that Zn₃N₂ films are prone to oxidation in ambient conditions. The oxide formation process is not self-limiting and can lead to the complete conversion of Zn₃N₂ to oxides or hydroxides if given enough time.^{13,16,32} This poor stability of Zn₃N₂ films is problematic in research studies as care has to be taken to minimize any effects of oxidation in evaluating their properties, such as determining the bandgap. In addition, it provides a challenge for potential applications of Zn₃N₂ in semiconductor devices because Zn₃N₂ layers exposed to air will have a short lifetime. For this reason, means of stabilizing Zn₃N₂ films are highly desirable. Previous studies have

reported that an intentionally grown oxide prevents oxidation in the bulk Zn₃N₂ layer by acting as a barrier.⁹ In this paper, we investigate the effects of thermal annealing on the ambient stability of the as-deposited Zn₃N₂ thin films. While thermal annealing of Zn₃N₂ films under a flow of oxygen has been investigated as a method to thermally oxidize Zn₃N₂, thermal annealing to reduce ambient oxidation has not been investigated.^{33–36} We report a remarkable improvement in ambient stability, achieved by annealing the as-deposited Zn₃N₂ films in a nitrogen atmosphere. We explain the observed improvements in ambient stability through a proposed mechanism for the oxidation process itself in these films.

EXPERIMENTAL DETAILS

Zn₃N₂ films were deposited on unheated glass substrates by DC sputtering of a Zn target (99.999%) in N₂ plasma in a Denton Vacuum Explorer. A N₂ flow rate of 45 sccm (99.999% purity) and a sputter power of 60 W were maintained during deposition. The base pressure in the sputter chamber was 6×10^{-7} Torr. Prior to each deposition, the N₂ gas line was purged at a flow rate of 100 sccm for 5 min. A 10-min pre-sputter process was applied to

ensure stable sputtering conditions before opening the main shutter. Five samples from the same sputtering experiment (75 ± 2 nm) were annealed in a rapid thermal annealer for 60 s at temperatures between 200°C and 400°C under flowing nitrogen gas to investigate the effects of annealing temperature on the properties of the Zn_3N_2 films. Optical measurements (transmittance, reflectance, and spectroscopic ellipsometry) were performed within minutes of exposure of the films to an ambient atmosphere. The annealed samples were also characterized by spectroscopic ellipsometry, and all samples were monitored for several months to evaluate their stability. All optical measurements were performed on a J. A. Woollam Variable Angle Spectroscopic Ellipsometry (WVASE) ellipsometer, and the experimental data were modeled using the commercial WVASE software. The properties of the semiconductor layers were modeled using a Herzinger–Johs parameterized function.³⁷ A set of thicker samples (700 nm) was deposited and annealed with the same process to investigate the effects of annealing on the crystal structure of the Zn_3N_2 films by X-Ray Diffraction (XRD) measurements. All samples were stored in a cleanroom environment with regulated humidity and temperature levels for the duration of this study.

RESULTS AND DISCUSSION

It was initially observed that thermal annealing of Zn_3N_2 films under nitrogen improved their ambient stability, making the films less prone to oxidation. This is demonstrated in Figs. 1(a) and 1(b), which shows the optical transmittance of an as-deposited sample and a sample annealed at 300°C , both monitored for a period of up to 18 weeks. The as-deposited Zn_3N_2 film was fully oxidized within 8 weeks, becoming transparent. In contrast, the annealed film showed no signs of oxidation over the full 18-week period. A cross-sectional SEM image of the annealed film after further exposure to ambient is shown in Fig. 1(c). The SEM image showed two clearly distinct layers: an oxide layer at the surface and a polycrystalline layer underneath it, followed by the amorphous substrate. Therefore, it was concluded that the annealed Zn_3N_2 film had been partially oxidized, although the oxide had been formed at a much slower rate.

To investigate the effect of annealing temperature on the rate of oxidation, a degradation study was performed on thin films (75 ± 2 nm) using spectroscopic ellipsometry measurements. Thinner films were selected for this study because they exhibited a very smooth surface. The details of the ellipsometric model that was used are discussed briefly in this section. Based on the observation in Fig. 1(c) of a multilayer structure produced through oxidation, we used a three-layer structure consisting of (a) the glass substrate, (b) the Zn_3N_2 layer, and (c) the oxide layer. The optical properties of the oxide layer were determined by fitting the model to the measurements of fully oxidized films. The properties of the Zn_3N_2 layers were determined by fitting the model to the measurements performed immediately after deposition and annealing. The refractive index and extinction coefficient obtained for the Zn_3N_2 layers are shown in Figs. 2(a) and 2(b), respectively. The obtained optical properties are in agreement with the expected values for both Zn_3N_2 ^{13,15,38} and $\text{ZnO}/\text{Zn}(\text{OH})_2$ (not shown here; bandgap of ~ 3.4 eV, refractive index of 1.6–1.8).¹³ It is noted that the optical properties of the Zn_3N_2 layers shift with annealing temperature. Specifically, the absorption onset red shifts from ~ 1.4 eV to ~ 1.0 eV,

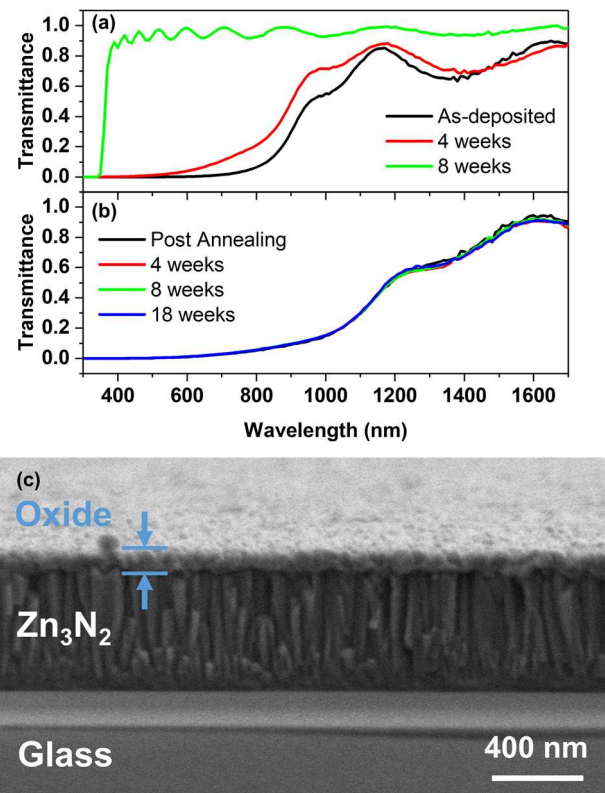


FIG. 1. Transmittance spectra of (a) an as-deposited and (b) an annealed 700 nm Zn_3N_2 film for up to 18 weeks. (c) Scanning electron microscopy image of a partially oxidized Zn_3N_2 film.

and the refractive index decreases from 2.6 to 2.4. This trend indicates a change in the band structure of the material, which was attributed to changes in the structure of the films after annealing, discussed later in this paper.

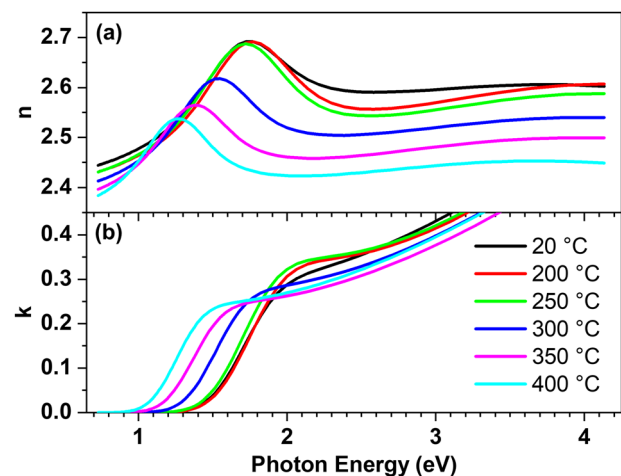


FIG. 2. (a) Refractive index, n , and (b) extinction coefficient, k , of the Zn_3N_2 layer obtained by spectroscopic ellipsometry for different annealing temperatures.

The thicknesses of the Zn_3N_2 and oxide layers measured by ellipsometry are shown in Figs. 3(a) and 3(b) for up to 682 days after deposition. The as-deposited 75 nm film examined here was fully oxidized within 3 days of exposure to ambient. However, films annealed under nitrogen became increasingly more stable with increasing annealing temperature. At annealing temperatures of 350–400 °C, the films showed little or no signs of oxidation for up to 300 days after deposition. To explicitly illustrate the dramatic effect of annealing on stability, the time to full oxidation of the films was measured and is plotted as a function of annealing temperature in Fig. 3(c). The time to full oxidation increases from 3 to 1818 days for the as-deposited film and the sample annealed at 350 °C. The average rates of oxidation are listed in Table I. The measured oxidation rate for the most durable samples is 10^{-2} – 10^{-1} nm/day, which is several orders of magnitude lower than the as-deposited sample (order of 10 nm/day).

Further analysis of the data presented in Fig. 3(a) was performed to shed light on the underlying mechanism behind the

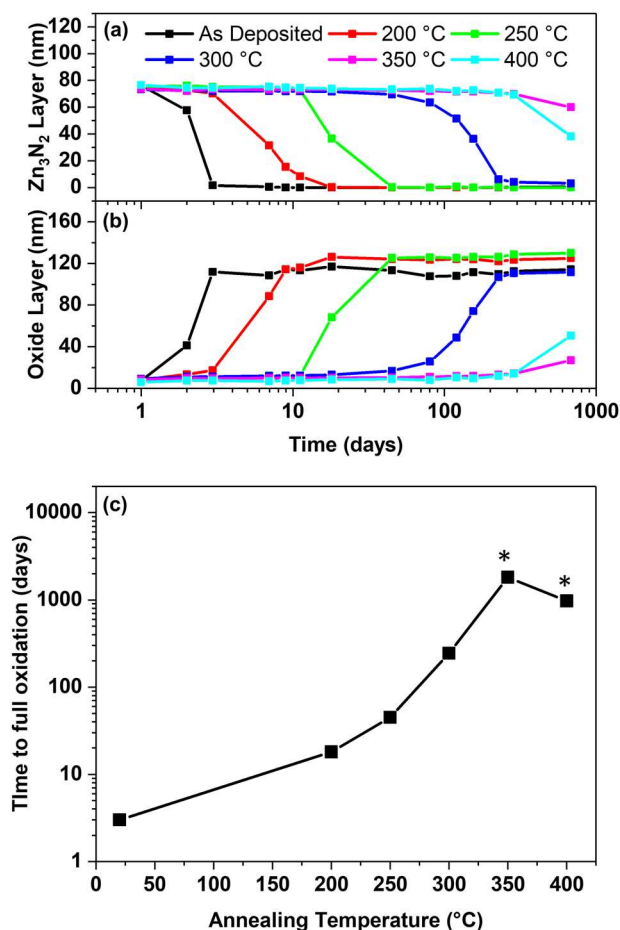


FIG. 3. Thickness of (a) the Zn_3N_2 layer and (b) oxide layers over several months for annealed samples. (c) Lifetime of the Zn_3N_2 layer as a function of annealing temperature. The data points marked with * were extrapolated based on the oxidation rates measured in this study.

TABLE I. Time to full oxidation and oxidation rates for the annealed Zn_3N_2 films. Data indicated with an asterisk (*) were extrapolated based on available data.

Annealing conditions	Surface oxidation duration (days)	Time to full oxidation (days)	Bulk oxidation rate (nm/day)
As deposited	<1	3	3.5×10^1
200 °C	3	18	4.7×10^0
250 °C	13	36	3.0×10^0
300 °C	27	257	3.0×10^{-1}
350 °C	228	1818*	4.4×10^{-2}
400 °C	228	972*	9.4×10^{-2}

improved stability. Two regions were identified in the oxidation process: an initial step with a slow oxidation rate (surface oxidation) and a subsequent step with an increased oxidation rate in the bulk of the films (bulk oxidation). The following mechanism is proposed to explain the observed results. Two reactions between Zn_3N_2 , O_2 , and H_2O species are commonly used in the literature to describe the process of oxidation,



Following the initial formation of a native oxide on the Zn_3N_2 surface, reactions (1) and (2) indicate that further oxidation requires two steps: (a) the diffusion of O_2 and H_2O species through the oxide layer and onto the Zn_3N_2 surface, followed by (b) the reaction of the diffused species with the Zn_3N_2 surface, which results in the further growth of the oxide layer. Therefore, the improved stability with annealing temperature can be attributed to an improvement in the structural quality of the surface oxide layer, which makes it less permeable to O_2 and H_2O species. Over time, the newly formed oxide in step (b) likely damages the quality of the surface oxide and increases the average reaction rate. However, the diffusion of oxidizing species onto the Zn_3N_2 surface remains a rate-limiting step, as indicated by the very low oxidation rate throughout the entire oxidation process. The present study indicates that an annealing temperature of 350 °C is optimum for the observed improvement in stability, which suggests that the capping oxide layer begins to deteriorate at higher temperatures. Temperatures in the range of 400–600 °C are used in the literature to thermally oxidize Zn_3N_2 films.^{33,35,36} Therefore, it is likely that in the absence of oxygen, the oxide layer begins to crack in this temperature range, having an adverse effect on the stability of the Zn_3N_2 film.

To investigate the changes observed in the optical properties of the annealed Zn_3N_2 layers in Fig. 2(b), the diffraction patterns of the annealed films were measured by XRD. The 75 nm films were almost amorphous and showed some improvement in crystallinity as a result of the thermal annealing process. The 700 nm films exhibited the (400) and (440) diffraction peaks, which are typically the main features in polycrystalline Zn_3N_2 films.^{13,14,39} The (400) diffraction peak is shown in Fig. 4 for a set of samples annealed at 200 °C, 300 °C, and 400 °C. The graph shows that the (400) peak shifted to higher angles when annealed at high temperatures. This trend was

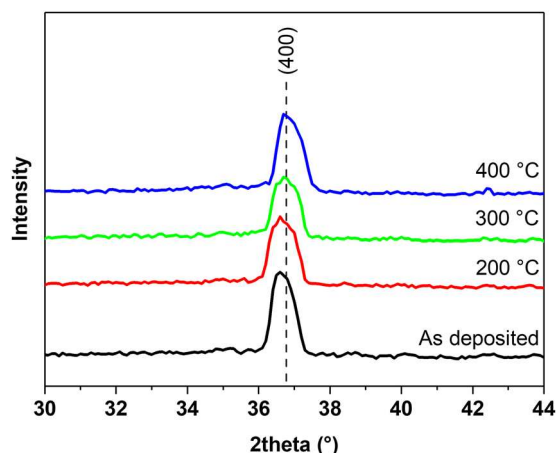


FIG. 4. X-ray diffraction scans of the (400) peak for Zn_3N_2 samples annealed at different temperatures. The dashed line shows the position of the (400) peak based on crystallographic data.³⁹

consistent in all Zn_3N_2 films examined here. Using Bragg's law of diffraction, this shift is attributed to a decrease in the lattice parameter from 9.78 Å to 9.74 Å. This change in the lattice parameter indicates changes in residual stress within the polycrystalline films caused by a mismatch of the thermal expansion coefficients between the film and the substrate.⁴⁰ The changes in strain observed for the Zn_3N_2 structure correlate with the shift in the optical bandgap of the Zn_3N_2 films, as shown in Fig. 2(b). While it is generally known that lattice compression or expansion can cause the bandgap of semiconductors to shift,^{41–43} the magnitude of the bandgap shift is very large for the samples examined in this study (~400 meV). However, the changes observed in the diffraction pattern indicate that the structure of the nanocrystalline Zn_3N_2 films is affected by the thermal annealing process. The authors believed that improvements in the structure of the Zn_3N_2 films, e.g., possibly a combination of bonding changes in grain boundaries, strain relaxation, and changes in stoichiometry such as evaporation of excess Zn, may explain the observed redshift of the bandgap. The range of optical bandgaps reported here as a function of annealing temperature covers a significant portion of the narrow bandgaps often reported in the literature for Zn_3N_2 (1.2–1.5 eV).^{9,13–22} Therefore, it is argued that variations of the Zn_3N_2 bandgap within this range, which are commonly found in the literature, may be the result of similar variations in structure due to processing or growth conditions.

CONCLUSION

In conclusion, this study discusses the effects of *ex situ* thermal annealing on the stability and other properties of Zn_3N_2 films. It was found that the ambient stability of films annealed in nitrogen increased significantly. The annealed Zn_3N_2 samples were increasingly more stable up to an annealing temperature of 350 °C. A mechanism is proposed to explain these observations, which involves the stabilization of the native oxide of Zn_3N_2 films. In the as-deposited samples, the native oxide grows uncontrollably, depleting entirely

the Zn_3N_2 layer (up to several hundred nanometers). Post-annealing, the native oxide is stabilized and acts as a capping layer, significantly slowing down the oxidation rate. The dramatic improvement in the stability of Zn_3N_2 films demonstrated here provides a simple method to utilize the native oxide of Zn_3N_2 films without growing additional capping layers. This solves a major practical challenge in the research and development of Zn_3N_2 , and technologies related to it.

ACKNOWLEDGMENTS

The authors acknowledge funding from the EPSRC (Engineering and Physical Science Research Council; Grant No. EP/M507611/1) and Johnson Matthey PLC (Award No. 14550005). The financial support from these parties is highly appreciated.

DATA AVAILABILITY

The data that support the findings of this study are openly available in the University of Sheffield data repository at <https://doi.org/10.15131/shef.data.10049825> (see Ref. 44).

REFERENCES

- S. R. Bhattacharyya, R. Ayouchi, M. Pinnisch, and R. Schwarz, *Phys. Status Solidi C* **9**, 469 (2012).
- C. G. Núñez, J. Jiménez-Trillo, M. G. Vélez, J. Piqueras, J. L. Pau, C. Coya, and A. L. Álvarez, *Appl. Surf. Sci.* **285**(Part B), 783 (2013).
- S.-H. Yoo, A. Walsh, D. O. Scanlon, and A. Soon, *RSC Adv.* **4**, 3306 (2014).
- N. Jiang, J. L. Roehl, S. V. Khare, D. G. Georgiev, and A. H. Jayatissa, *Thin Solid Films* **564**, 331 (2014).
- P.-C. Wei, S.-C. Tong, C.-M. Tseng, C.-C. Chang, C.-H. Hsu, and J.-L. Shen, *J. Appl. Phys.* **116**, 143507 (2014).
- X. Cao, Y. Ninomiya, and N. Yamada, *Phys. Status Solidi A* **214**, 1600472 (2017).
- M. B. Haider, *Nanoscale Res. Lett.* **12**, 5 (2017).
- M. Ullah, G. Murtaza, M. Yaseen, and S. A. Khan, *J. Alloys Compounds* **728**, 1226 (2017).
- C. G. Núñez, J. L. Pau, E. Ruiz, and J. Piqueras, *Appl. Phys. Lett.* **101**, 253501 (2012).
- R. Ahumada-Lazo, S. M. Fairclough, S. J. O. Hardman, P. N. Taylor, M. Green, S. J. Haigh, R. Saran, R. J. Curry, and D. J. Binks, *ACS Appl. Nano Mater.* **2**, 7214 (2019).
- P. N. Taylor, M. A. Schreuder, T. M. Smeeton, A. J. D. Grundy, J. A. R. Dimmock, S. E. Hooper, J. Heffernan, and M. Kauer, *J. Mater. Chem. C* **2**, 4379 (2014).
- Y. Wang, T. Ohsawa, Y. Kumagai, K. Harada, F. Oba, and N. Ohashi, *Appl. Phys. Lett.* **115**, 092104 (2019).
- A. Trapalis, J. Heffernan, I. Farrer, J. Sharman, and A. Kean, *J. Appl. Phys.* **120**, 205102 (2016).
- A. Trapalis, I. Farrer, K. Kennedy, A. Kean, J. Sharman, and J. Heffernan, *Appl. Phys. Lett.* **111**, 122105 (2017).
- C. G. Núñez, J. L. Pau, M. J. Hernández, M. Cervera, and J. Piqueras, *Appl. Phys. Lett.* **99**, 232112 (2011).
- C. G. Núñez, J. L. Pau, M. J. Hernández, M. Cervera, E. Ruiz, and J. Piqueras, *Thin Solid Films* **520**, 1924 (2012).
- M. Futsuhara, K. Yoshioka, and O. Takai, *Thin Solid Films* **322**, 274 (1998).
- T. Yang, Z. Zhang, Y. Li, M. Lv, S. Song, Z. Wu, J. Yan, and S. Han, *Appl. Surf. Sci.* **255**, 3544 (2009).
- G. Z. Xing, D. D. Wang, B. Yao, L. F. N. A. Qune, T. Yang, Q. He, J. H. Yang, and L. L. Yang, *J. Appl. Phys.* **108**, 083710 (2010).

- ²⁰A. H. Jayatissa and T. Wen, *Surf. Coat. Technol.* **211**, 163 (2012).
- ²¹A. H. Jayatissa, T. Wen, and M. Gautam, *J. Phys. D: Appl. Phys.* **45**, 045402 (2012).
- ²²T. Wen, M. Gautam, A. M. Soleimanpour, and A. H. Jayatissa, *Mater. Sci. Semicond. Process.* **16**, 318 (2013).
- ²³P. Wu, X. Cao, T. Tiedje, and N. Yamada, *Mater. Lett.* **236**, 649 (2019).
- ²⁴X. Cao, A. Sato, Y. Ninomiya, and N. Yamada, *J. Phys. Chem. C* **119**, 5327 (2015).
- ²⁵X. Cao, Y. Yamaguchi, Y. Ninomiya, and N. Yamada, *J. Appl. Phys.* **119**, 025104 (2016).
- ²⁶S. Sinha, D. Choudhury, G. Rajaraman, and S. K. Sarkar, *RSC Adv.* **5**, 22712 (2015).
- ²⁷S. Sinha and S. K. Sarkar, *RSC Adv.* **4**, 47177 (2014).
- ²⁸S. Simi, I. Navas, R. Vinodkumar, S. R. Chalana, M. Gangrade, V. Ganesan, and V. P. M. Pillai, *Appl. Surf. Sci.* **257**, 9269 (2011).
- ²⁹R. Ayouchi, C. Casteleiro, L. Santos, and R. Schwarz, *Phys. Status Solidi C* **7**, 2294 (2010).
- ³⁰N. Yamada, K. Watarai, T. Yamaguchi, A. Sato, and Y. Ninomiya, *Jpn. J. Appl. Phys., Part 1* **53**, 05FX01 (2014).
- ³¹V. Şenay, S. Özen, and T. Aydoğmuş, *Optik* **191**, 15 (2019).
- ³²C. G. Núñez, J. L. Pau, M. J. Hernández, M. Cervera, E. Ruíz, and J. Piqueras, *Thin Solid Films* **522**, 208 (2012).
- ³³C. Wang, Z. Ji, K. Liu, Y. Xiang, and Z. Ye, *J. Cryst. Growth* **259**, 279 (2003).
- ³⁴D. Wang, Y. C. Liu, R. Mu, J. Y. Zhang, Y. M. Lu, D. Z. Shen, and X. W. Fan, *J. Phys.: Condens. Matter* **16**, 4635 (2004).
- ³⁵E. Kaminska, A. Piotrowska, J. Kossut, A. Barcz, R. Butkute, W. Dobrowolski, E. Dynowska, R. Jakiela, E. Przedziecka, R. Lukasiewicz, M. Aleszkiewicz, P. Wojnar, and E. Kowalczyk, *Solid State Commun.* **135**, 11 (2005).
- ³⁶J. Yu-Ping, Z. Bin, W. Jian-Zhong, and S. Li-Qun, *Chin. Phys. Lett.* **33**, 058101 (2016).
- ³⁷B. Johs, C. M. Herzinger, J. H. Dinan, A. Cornfeld, and J. D. Benson, *Thin Solid Films* **313**, 137 (1998).
- ³⁸N. Jiang, D. G. Georgiev, A. H. Jayatissa, R. W. Collins, J. Chen, and E. McCullen, *J. Phys. D: Appl. Phys.* **45**, 135101 (2012).
- ³⁹D. E. Partin, D. J. Williams, and M. O’Keeffe, *J. Solid State Chem.* **132**, 56 (1997).
- ⁴⁰E. Chason and P. R. Guduru, *J. Appl. Phys.* **119**, 191101 (2016).
- ⁴¹M. Devika, N. K. Reddy, F. Patolsky, K. Ramesh, and K. R. Gunasekhar, *Appl. Phys. Lett.* **95**, 261907 (2009).
- ⁴²Z. Zhu, A. Zhang, G. Ouyang, and G. Yang, *J. Phys. Chem. C* **115**, 6462 (2011).
- ⁴³C. Feng, J. Duan, and G. Liu, *Mater. Res. Express* **2**, 045008 (2015).
- ⁴⁴Dataset: A. Trapalis, I. Farrer, K. Kennedy, A. Kean, J. Sharman, and J. Heffernan (2020). “Data and figures related to publication: Improved ambient stability of thermally annealed Zinc Nitride thin films,” University of Sheffield. <https://doi.org/10.15131/shef.data.10049825>